RESEARCH ARTICLE

JOR *Spine* OPEN ACCESS

TRPV4 mediates cell damage induced by hyperphysiological compression and regulates COX2/PGE2 in intervertebral discs

Elena Cambria[1] [ID] | Sally Heusser[1] | Ariane C. Scheuren[1] | Wai Kit Tam[2] |
Agnieszka A. Karol[3] | Wolfgang Hitzl[4,5,6] | Victor Y. Leung[2] | Ralph Müller[1] |
Stephen J. Ferguson[1] | Karin Wuertz-Kozak[1,7,8] [ID]

[1]Institute for Biomechanics, ETH Zurich, Zurich, Switzerland

[2]Department of Orthopaedics and Traumatology, The University of Hong Kong, Pokfulam, Hong Kong

[3]Musculoskeletal Research Unit (MSRU), Department of Molecular Mechanisms of Disease (DMMD), Vetsuisse Faculty, University of Zurich, Zurich, Switzerland

[4]Research Office (Biostatistics), Paracelsus Medical University, Salzburg, Austria

[5]Department of Ophthalmology and Optometry, Paracelsus Medical University, Salzburg, Austria

[6]Research Program Experimental Ophthalmology and Glaucoma Research, Paracelsus Medical University, Salzburg, Austria

[7]Department of Biomedical Engineering, Rochester Institute of Technology, Rochester, New York

[8]Spine Center, Schön Klinik München Harlaching, Academic Teaching Hospital and Spine Research Institute of the Paracelsus Private Medical University Salzburg (Austria), Munich, Germany

Correspondence
Elena Cambria, Institute for Biomechanics, D-HEST ETH Zurich, Hönggerbergring 64, HPP O13, 8093 Zurich, Switzerland.
Email: ecambria@ethz.ch

Abstract

Background: Aberrant mechanical loading of the spine causes intervertebral disc (IVD) degeneration and low back pain. Current therapies do not target the mediators of the underlying mechanosensing and mechanotransduction pathways, as these are poorly understood. This study investigated the role of the mechanosensitive transient receptor potential vanilloid 4 (TRPV4) ion channel in dynamic compression of bovine nucleus pulposus (NP) cells in vitro and mouse IVDs in vivo.

Methods: Degenerative changes and the expression of the inflammatory mediator cyclooxygenase 2 (COX2) were examined histologically in the IVDs of mouse tails that were dynamically compressed at a short repetitive hyperphysiological regime (vs sham). Bovine NP cells embedded in an agarose-collagen hydrogel were dynamically compressed at a hyperphysiological regime in the presence or absence of the selective TRPV4 antagonist GSK2193874. Lactate dehydrogenase (LDH) and prostaglandin E2 (PGE2) release, as well as phosphorylation of mitogen-activated protein kinases (MAPKs), were analyzed. Degenerative changes and COX2 expression were further evaluated in the IVDs of trpv4-deficient mice (vs wild-type; WT).

Results: Dynamic compression caused IVD degeneration in vivo as previously shown but did not affect COX2 expression. Dynamic compression significantly augmented LDH and PGE2 releases in vitro, which were significantly reduced by TRPV4 inhibition. Moreover, TRPV4 inhibition during dynamic compression increased the activation of the extracellular signal-regulated kinases 1/2 (ERK) MAPK pathway by 3.13-fold compared to non-compressed samples. Trpv4-deficient mice displayed mild IVD degeneration and decreased COX2 expression compared to WT mice.

Conclusions: TRPV4 therefore regulates COX2/PGE2 and mediates cell damage induced by hyperphysiological dynamic compression, possibly via ERK. Targeted TRPV4 inhibition or knockdown might thus constitute promising therapeutic approaches to treat patients suffering from IVD pathologies caused by aberrant mechanical stress.

1 | INTRODUCTION

Intervertebral disc (IVD) degeneration, leading to IVD structural failure, causes degenerative disc disease (DDD) when it is accompanied and exacerbated by inflammation and nociception.[1,2] DDD is the main cause of low back pain (LBP), which is the leading cause of disability globally.[3,4] Aberrant mechanical loading of the spine is a recognized cause of IVD degeneration and LBP.[5,6] However, at the molecular level, the underlying mechanosensing and mechanotransduction pathways are poorly understood. As a result, current treatments of LBP, such as anti-inflammatory drugs, do not specifically target mediators of mechanotransduction pathways. A better understanding of the molecular mechanisms leading from hyperphysiological mechanical loading to IVD degeneration and inflammation would reveal novel, and possibly more effective, therapeutic targets.

IVDs are continually subjected to mechanical stimulation via spinal flexion, extension, torsion, and muscle activation during daily activities.[7] The well-hydrated nucleus pulposus (NP) in the middle of the IVD primarily sustains compressive loads, hydrostatic and osmotic pressures, while the surrounding annulus fibrosus (AF) is mostly exposed to tensile stress.[7] IVD homeostasis is dependent on a physiological level of mechanical stimulation, which promotes solute transport and cell metabolism.[5] However, hyperphysiological mechanical stress induces harmful structural, cellular, and molecular changes in the IVDs.[5,7] Several studies have focused on the investigation of compressive stimuli both in vivo and in vitro (reviewed in[5,7]). It was shown that hyperphysiological dynamic compression (at high magnitude, frequency, or duration) causes cell death,[8-10] decreased expression of anabolic genes (collagens and proteoglycans),[11-13] as well as increased expression of matrix-degrading enzymes (MMPs, ADAMTs)[11,13-16] and pro-inflammatory cytokines.[9] These effects might be mediated by mitogen-activated protein kinase (MAPK: extracellular signal-regulated kinases 1/2 (ERK 1/2), p38 and Jun-N-terminal kinase (JNK)) signaling pathways,[17,18] while the initial mechanosensing mechanisms might involve integrins, purinergic signaling, and ion channels, including transient receptor potential (TRP) channels.[7,17] Nevertheless, the exact mechanosensing and mechanotransductive mechanisms in IVD cells are currently unknown.

TRP ion channels are non-selective calcium-permeable transmembrane channels. They are of particular interest in the context of IVD research, as they sense variations in several factors that are altered during IVD degeneration: pH, oxidative and mechanical stress.[19] The TRP super-family is composed of six sub-families in mammals: TRPC (canonical), TRPV (vanilloid), TRPM (melastatin), TRPP (polycystin), TRPML (mucolipin), and TRPA (ankyrin).[19] Several studies have recently investigated the expression and function of TRP channels in the IVD.[20-24] The mechanosensitive member 4 of the vanilloid subfamily (TRPV4) is especially intriguing for the study of load-mediated IVD degeneration and LBP. TRPV4 was shown to transduce physiological dynamic compression in porcine articular chondrocytes.[25] Moreover, cartilage-specific TRPV4 knockout in mice reduced age-related osteoarthritis.[26] In the IVD field, reduced osmolarity was shown to increase TRPV4 expression and pro-inflammatory cytokines in bovine NP cells.[20] Moreover, our group has recently shown that TRPV4 transduces hyperphysiological mechanical loading into increased COX2 gene expression and PGE2 release in human AF cells cyclically stretched in two dimensions (2D).[24]

Building on these results, we hypothesized that hyperphysiological dynamic compression induces IVD degeneration, cell damage and increased COX2/PGE2 expression, and that TRPV4 mediates these effects in murine IVDs and bovine NP cells embedded in a previously developed three-dimensional (3D) matrix.[27] This agarose-collagen composite hydrogel mimics the 3D aspect of the NP with its non-fibrillar matrix (proteoglycans and glycosaminoglycans) and collagen fibers, combines mechanical strength and biofunctionality, and is thus suitable for mechanotransduction studies.[27]

2 | MATERIALS AND METHODS

2.1 | Compressed murine tails for histology

Sham and compressed mouse tails of 15-week-old female C57BL/6J mice (Charles River Laboratories, France) were provided by the Laboratory for Bone Biomechanics at ETH Zurich, Switzerland, as a by-product of another study.[28] The sixth caudal vertebra (C6) and the IVDs between C5 and C6, and C6 and C7 were dynamically compressed (8 N, 2 Hz, sine wave, 5 min, 3× per week over 4 weeks) via two stainless steel pins inserted in C5 and C7, as described elsewhere.[28,29] We estimated the pressure by dividing the load of 8 N by a mean mouse disc area. The mean mouse disc cross-sectional area was computed from sample-specific discs[29] estimated from the micro-CT images of eight mice from the compression group, resulting in a mean area of 1.275 mm2 (SD = 0.059 mm^2). The resulting estimated pressure is therefore 6.274 MPa. Sham mice received pins and their tails were fixed in the loading device but were not dynamically compressed. Immediately after euthanasia, the tails were dissected, rinsed in phosphate buffered saline (PBS), and fixed in 4% paraformaldehyde solution for 24 h. The fixed tails were washed in PBS and decalcified in 12.5% ethylene-diamine-tetra-acetic acid (EDTA) in PBS at 4°C for 10 days. The decalcified samples were washed in PBS and placed into 70% ethanol at 4°C until paraffin embedding. Paraffin blocks were sectioned at 5 μm thickness. The experiments were carried out in strict accordance with the recommendations and regulations in the

Animal Welfare Ordinance (TSchV 455.1) of the Swiss Federal Food Safety and Veterinary Office (license number 262/2016).

2.2 | FAST histological staining

IVD degeneration was assessed via a multi-dye FAST (Fast Green, Alcian Blue, Safranin-O, and Tartrazine) histological staining, as previously described.[30] Briefly, paraffin sections were dewaxed in xylene and then rehydrated successively in 70% ethanol, 30% ethanol, and distilled water. The sections were first stained with 1% Alcian Blue 8GX (A3157, Sigma-Aldrich) at pH 1.0 for 2.5 min, followed by 0.1% Safranin-O (S8884, Sigma-Aldrich) for 3 min. Color differentiation was performed in 25% ethanol for 15 s. The sections were then stained with 0.08% Tartrazine (T0388, Sigma) in 0.25% acetic acid for 15 s and finally counterstained with 0.01% Fast Green (F7258, Sigma) solution for 5 min. Sections were air-dried, mounted in DePeX (BDH Laboratory; Poole, UK), and examined under a Nikon Eclipse 80i microscope (Tokyo, Japan). IVD degeneration was evaluated semi-quantitatively according to the criteria of Tam et al.[31]

2.3 | COX2 immunohistochemistry

Histological sections were deparaffinized and a heat-mediated antigen retrieval was conducted (PT-Link, 95°C, 20 min, in citrate buffer pH 6.0). Subsequently, the sections were immunolabeled with a primary antibody recognizing COX2 protein expression (ab15191, abcam, LOT #GR299479-4, dilution 1:500) for 1 h at 37°C. Secondary anti-mouse/rabbit IgG (Dako EnVisionTM+ Dual Link System-HRP) was applied (1:200 dilution) for 30 min at room temperature (RT), followed by the amino-9-ethyl-carbazole (AEC) substrate kit (Dako) as a chromogen. Finally, the sections were counter-stained with Gill's

TABLE 1 Allred scoring system

Score A	Percentage of positive cells
0	0
1	<1
2	1 to 10
3	11 to 33
4	34 to 66
5	≥67
Score B	**Signal intensity**
0	None
1	Weak
2	Intermediate
3	Strong
Final score A + B	**Interpretation**
0–2	Negative
3–8	Positive

hematoxylin for 3 min and cover-slipped with an aqueous mounting medium (Glicerine, Sigma-Aldrich). Positive controls were performed by staining sections of mouse brain, which expresses COX2 (Supplementary Figure S1). For the "no primary antibody" negative controls, only the diluent of the primary antibody (PBS) was used instead of the primary antibody. This was followed by the application of the secondary antibody and detection reagents as usual (Supplementary Figure S1). Sections were evaluated semi-quantitatively with the Allred score according to percentage of positively stained cells (score A) and immunohistochemical signal intensity (score B) (Table 1).[32] The two scores were added together for a final score ranging from 0 to 8. Final scores of 0 to 2 were considered negative and scores of 3 to 8 were considered positive.

2.4 | Bovine NP cell isolation and culture

Bovine NP cell isolation and culture were performed as described previously.[27] Briefly, tails from 18-24-month-old cows were purchased from the local slaughterhouse and carefully dissected to separate the NP from the AF of the IVDs. NP biopsies were minced and digested overnight at 37°C, 5% CO_2, using 0.4% collagenase NB4 (17454.01, Serva) and 0.2% dispase II (04942078001, Roche) dissolved in PBS $1\times$ with 3% Antibiotic-Antimycotic (Anti-Anti; 15240-062, Gibco). The tissue digest was filtered, and NP cells were pelleted, washed with culture medium (Dulbecco's modified Eagle medium/F-12 Nutrient Mixture (DMEM/F12; 31330-038, Gibco), 10% fetal calf serum (FCS; F7524, Sigma-Aldrich) and 1% Anti-Anti), centrifuged, resuspended in culture medium and seeded in fibronectin-coated culture flasks. Cells were expanded to passage 1 to 2 at 37°C, 5% CO_2 and the medium was changed twice per week.

2.5 | Agarose-collagen hydrogel fabrication and culture

Bovine NP cells were embedded and cultured in agarose-collagen hydrogels as described previously.[27] Briefly, after trypsinization, pelleted NP cells were first resuspended in a 4 mg/mL collagen type I solution (5010, Advanced BioMatrix) prepared on ice at a density of 8×10^6 cells/mL. The solution was then mixed 1:1 with a 4% wt/vol agarose solution (5010, Lonza) kept at 60°C to obtain a final concentration of 4×10^6 cells/mL in agarose 2% wt/vol and collagen 2 mg/mL. Hydrogels (160 μL) were molded in silicon rings (inner Ø: 8 mm, outer Ø: 12 mm, height: 3 mm) for radial containment and placed between two microscope glass slides. Hydrogels were pre-cultured in 12-well plates at 37°C, 5% CO_2 in DMEM/F12 phenol red-free medium (11 039, Gibco), supplemented with 10% FCS, 0.1% ampicillin (A0839, AppliChem) and 50 μg/mL L-ascorbic acid (A4544, Sigma-Aldrich) for 7 days before mechanical loading. The medium was changed every other day.

FIGURE 1 A, Bottom view of the MCTR device with its nine wells. B, Side view of one well containing one hydrogel in a silicone ring. When pressure is applied (pressurized air), an elastic membrane deforms and pushes a shuttle down, which compresses the construct. A magnet placed on top of the elastic membrane sticks to the shuttle. The magnetic field is used to determine the displacement of the constructs. Adapted from CellScale

2.6 | Cell-laden hydrogel dynamic compression

Four hours before compression, medium was changed to phenol red-free DMEM/F12 supplemented with 0.1% ampicillin, 50 μg/mL ascorbic acid, and 10% charcoal-stripped FCS (A3382101, Gibco). For dynamic compression, the hydrogels in silicon rings were transferred to the wells of a commercial compression device (MCTR, CellScale) in 1 mL of the above medium (Figure 1A,B). Hydrogels were dynamically compressed with a sine wave function at 0.5 Hz with a nominal force of 73 N and 13 N of pre-load for 1 h (unless otherwise stated) at 37°C, 5% CO_2. As the silicone ring dominates the stiffness, a strain of 20% can be inferred. Non-compressed hydrogels were kept in identical conditions in a 24-well plate.

2.6.1 | Harvesting time-point

After compression, the hydrogels were transferred with their conditioned medium to a 24-well plate and further cultured for 24 or 48 h for analysis of the conditioned medium.

2.6.2 | TRPV4 inhibition

Cell-laden hydrogels were pre-treated for 15 min with 0, 50, 100, or 200 nM of the selective TRPV4 antagonist GSK2193874 (17715, Cayman Chemical). The concentration of the vehicle (DMSO) was equalized in all chambers (0.002%). Hydrogels were subjected to dynamic compression for 1 h in the presence or absence of TRPV4 antagonist. After compression, the hydrogels were transferred with their conditioned medium to a 24-well plate and further cultured for 48 h for analysis of the conditioned medium.

2.6.3 | MAPK phosphorylation

Hydrogels were pre-treated for 15 min with 0, 50, 100, or 200 nM of GSK2193874 and compressed for 30 min in the presence or absence of TRPV4 antagonist. The loading duration was changed to 30 min because it was shown that the phosphorylation of MAPKs peaks

between 15 and 30 min of mechanical loading and then fades away in IVD cells.[33] Hydrogels were immediately processed for protein analysis. The lysates of two hydrogels per donor and per condition were pooled to reach sufficient protein amounts for Western blot.

2.7 | Lactate dehydrogenase assay

Lactate dehydrogenase (LDH) is a cytosolic enzyme present in most cell types. The LDH assay is a cytotoxicity assay that quantifies the leakage of LDH into the extracellular medium upon plasma membrane damage and cell death. As such, it is an indirect measure of cell viability. A low absorbance at 490 nm can be interpreted as high viability, while a high absorbance at 490 nm means low viability. Extracellular LDH was quantified using the colorimetric Pierce LDH Cytotoxicity Assay Kit (88954, Thermo Fisher Scientific) according to the manufacturer instructions. Samples (conditioned medium), blanks (medium used for compression), and the positive control of the kit were added in duplicates into a 96-well flat-bottom plate (50 μL/well). The reaction mixture was added (50 μL/well), and the plate was incubated at RT for 30 min protected from light. Stop solution was added (50 μL/well) and gently mixed. The absorbance was immediately measured at 490 nm with a reference at 680 nm using a plate reader (Infinite M200 PRO, TECAN). The average absorbance of the blanks was subtracted from the average absorbance of the samples.

2.8 | PGE2 enzyme-linked immunosorbent assay

A competitive inhibition PGE2 ELISA kit (RD-PGE2-Ge, Reddot Biotech) was used to quantify the levels of PGE2 in the conditioned medium according to the manufacturer instructions. Samples were used undiluted in duplicates. PGE2 concentrations are expressed relative to the concentration of the non-compressed control.

2.9 | Protein extraction and Western blot

Hydrogels were processed as described previously.[27] Briefly, hydrogels were cut into four pieces, washed with PBS 1×, snap-frozen in

liquid nitrogen, and lyophilized overnight. RIPA buffer supplemented with protease and phosphatase inhibitor cocktails (78430; 78428, Thermo Fisher Scientific) was used to lyse the hydrogels on ice (100 μL/gel) for 1 h. The lysates and the soaked hydrogels were centrifuged in NucleoSpin filter columns (740606, Macherey-Nagel) for 1 h at 4°C at 12'000 rpm. For all samples, 22.5 μL of lysate were mixed with 4× Laemmli buffer (1610747, Bio-Rad), heated at 95°C, and loaded onto a 4% to 20% gradient gel (4568093, Bio-Rad). Proteins were separated by electrophoresis in a Mini-PROTEAN Tetra Cell (Bio-Rad) and transferred to PVDF membranes (1704156, Bio-Rad). The membranes were washed with Tris Buffered Saline with 0.05% TWEEN 20 (TBS-T) and blocked for 2 h at RT with 5% skim milk in TBS-T. Primary antibodies (ERK1/2 (ERK): 9102; p-ERK: 9101; p38: 9212; p-p38: 9211; JNK: 9252; p-JNK: 9251; α-tubulin: 2144; Cell Signaling Technology) were applied 1:1000 in 5% BSA in TBS-T overnight at 4°C on a rocker. The membranes were washed with TBS-T and incubated for 1 h at RT on a rocker with the secondary antibody (anti-rabbit IgG HRP: 7074, Cell Signaling Technology) diluted 1:2000 in 5% skim milk in TBS-T. After washing with TBS-T, proteins were detected with a chemiluminescence substrate (34076, Thermo Fisher Scientific) on a ChemiDocTouch Imaging System (Bio-Rad). The density of the bands was semi-quantified on the ImageLab software (Bio-Rad). For each blot, the density of each band was normalized by the one of the non-compressed control. The ratio phosphorylated MAPKs/total MAPKs was calculated.

2.10 | Trpv4 knockout murine tails for histology

Tails from unloaded wild-type (WT) and trpv4 knockout (KO) C57BL/6J mice were kindly provided by the Laboratory of Ion Channel Research at KU Leuven, Belgium. The trpv4 KO strain Trpv4[tm1.1Ldtk34] was backcrossed at least ten times into the C57BL/6J background, and C57BL/6J mice were used as WT controls. Mice of all genotypes were housed under identical conditions, with a maximum of four animals per cage on a 12-hour light-dark cycle and with food and water ad libitum. Fifteen-week-old male mice were euthanized and the tails were dissected, fixed, and washed as described above, and decalcified in Morse's solution at 4°C for 3 days. The decalcified samples were processed and sectioned as described above. The experiments were approved by the KULeuven Ethical Committee under the project "in vitro", license number LA1210202.

2.11 | Statistical analysis

Data were checked for consistency and normality using skewness, kurtosis, and omnibus tests. Due to the small sample sizes, dependent bootstrap t-tests based on 10000 Monte Carlo samples were used. Repeated parametric ANOVAs and nonparametric ANOVA (Friedman aligned test) were used to test effects globally. In addition, for pairwise testing, classical dependent t-tests and nonparametric tests (Wilcoxon Signed test) and Quantile Sign test were used. All reported tests were two-sided, and P values <.05 were considered statistically significant. All statistical analyses were performed by using NCSS (NCSS 10, NCSS, LLC. Kaysville, UT), PASW 24 (IBM SPSS Statistics for Windows, Version 21.0., Armonk, NY) and StatXact (2013, Version 10.0.0, Cytel software cooperation, Cambridge, MA, USA).

3 | RESULTS

3.1 | Dynamic compression of murine IVDs causes mild degeneration in vivo

Dynamic compression was previously shown to induce IVD degeneration in vivo.[8,11,12,14,16] However the expression of COX2 has not been investigated. In a first step, we verified that dynamic compression causes structural and degenerative changes in mouse IVDs via a FAST histological staining. Sham IVDs showed a distinct and intact structure (Figure 2A) with a single NP cell mass surrounded by matrix (Figure 2A,B), a well-defined NP/AF boundary (Figure 2A,C), and concentric lamellae in the AF (Figure 2A,C). However, in dynamically compressed IVDs, the NP cell mass was mildly segregated, with the intercellular space taken up by matrix (Figure 2D,E). The NP/AF boundary was less clear (Figure 2D,F) with inner AF lamellae that were more spaced apart compared to sham (Figure 2F). Rounder chondrocyte-like cells were present in the AF and small clefts were present in the outer AF region (Figure 2F). Dynamic compression at 8 N, 2 Hz, 5 min 3× per week over 4 weeks, thus induces features of mild degeneration in mouse IVDs.

3.2 | Dynamic compression of murine IVDs does not affect COX2 expression in vivo

We previously showed that cyclic hyperphysiological stretching increases COX2 gene expression and the release of its product PGE2 in human AF cells.[24] In order to investigate the link between dynamic compression and inflammation, we performed immunohistochemistry (IHC) to detect COX2 expression in sham and compressed mouse IVDs in vivo. COX2 was constitutively expressed in the NP of sham IVDs (Figure 3A,B) and dynamic compression did not clearly affect COX2 expression (Figure 3C,D) (Table 2). COX2 was not expressed in the AF (Figure 3A,C). In Figure 3A, the AF was partially lost due to the harsh antigen retrieval protocol.

3.3 | Hyperphysiological dynamic compression increases LDH and PGE2 release in vitro

In the second part of the study, we aimed to verify in vitro the effects of hyperphysiological dynamic compression observed in vivo, and to investigate the potential role of TRPV4. Bovine NP cells were isolated and cultured in 3D agarose-collagen hydrogels.

Sham

(A)

(B)

NP

(C)

IAF   OAF

DC

(D)

(E)

NP

(F)

IAF   OAF
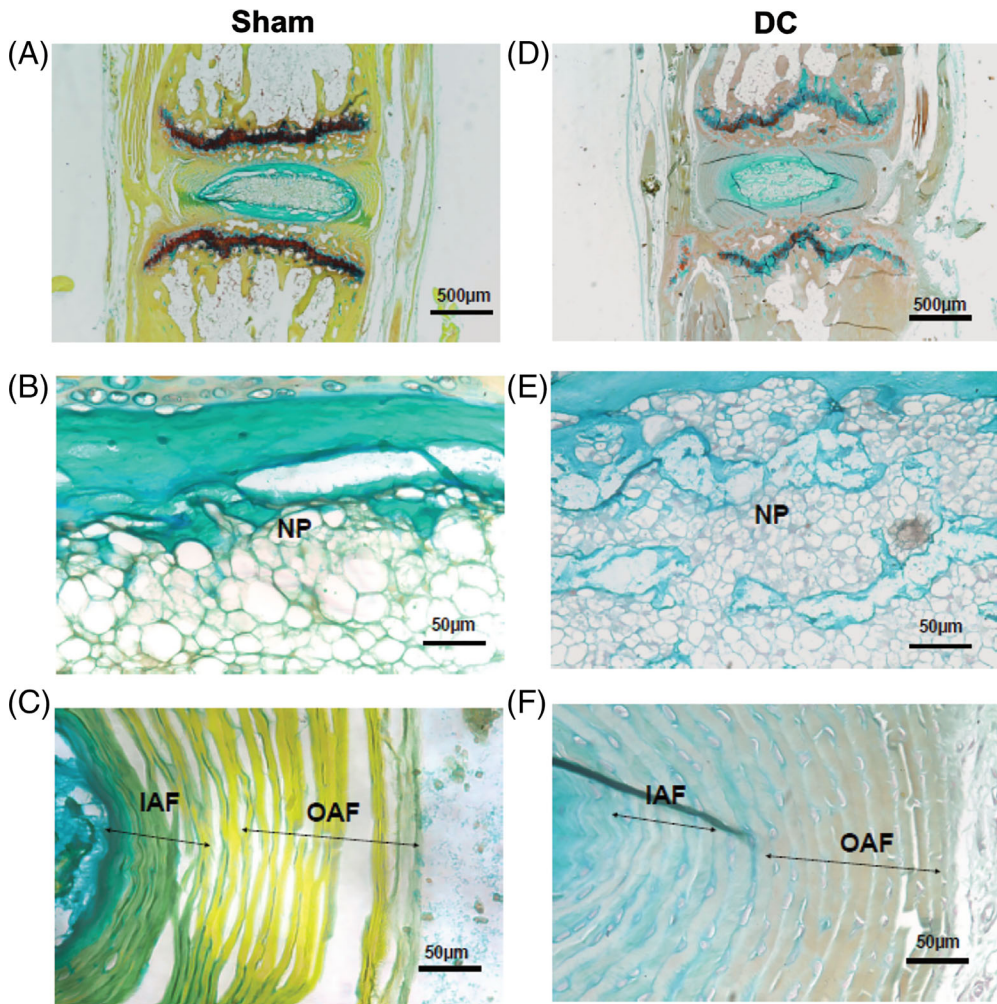
FIGURE 2 FAST staining of IVDs of sham, A-C, and dynamically compressed (DC; D-F) mouse tails. The nucleus pulposus (NP; B, E), inner and outer annulus fibrosus (IAF and OAF; C, F) are shown with a higher magnification. Scale bars: 500 μm in (A, D); 50 μm in B, E, and C, F. n = 2 in the sham group, n = 5 in the DC group

Sham

(A)

(B)

DC

(C)

(D)
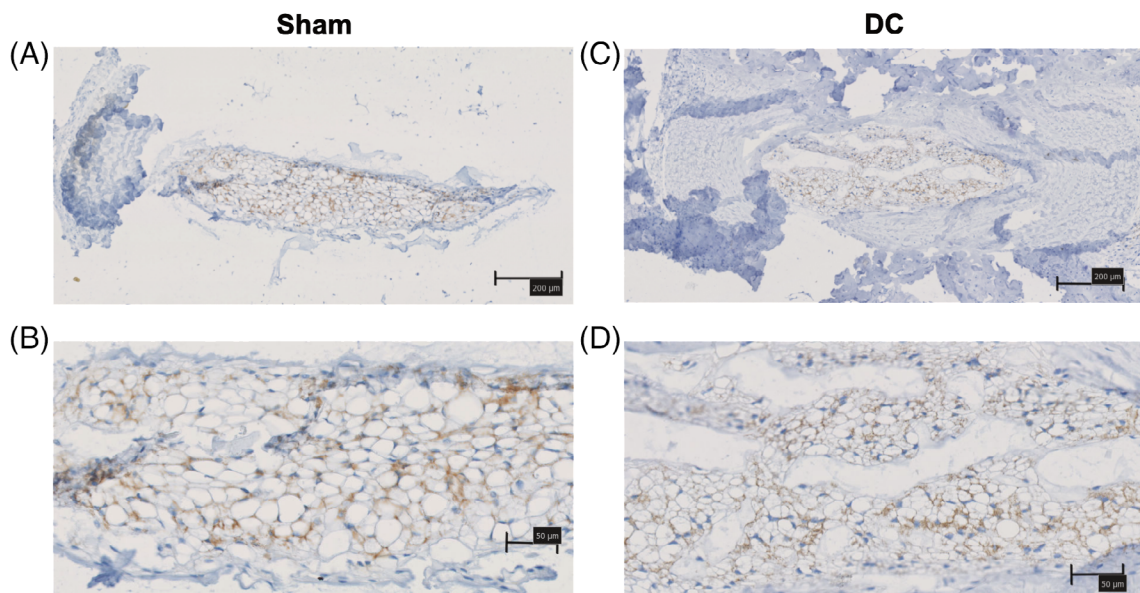
FIGURE 3 COX2 immunohistochemistry of IVDs of sham, A, B, and dynamically compressed (DC; C, D) mouse tails. Scale bars: 200 μm in A, C, and 50 μm in B, D. n = 2 in the sham group, n = 3 in the DC group

Cell-laden hydrogels were dynamically compressed for 1 h at 0.5 Hz at a hyperphysiological regime of 73 N (corresponding to 20% strain). In order to test the effect of hyperphysiological dynamic compression on cell damage and inflammation, the release of LDH and PGE2 (a product of COX2) was measured 24 and 48 h after the end of mechanical loading. No significant changes were observed after 24 h (Figure 4A,B). However, LDH release

considerably increased 48 h after compression compared to non-compressed cell-laden constructs (Figure 4A). Furthermore, a slight but statistically significant 1.14-fold augmentation in PGE2 release was observed in compressed hydrogels compared to controls after 48 h (Figure 4B). These data show that 1 h of hyperphysiological dynamic compression already induces NP cell damage and slight inflammation in vitro.

TABLE 2 Allred scoring of COX2 immunohistochemistry of IVDs of sham and dynamically compressed (DC) mouse tails

Sample	Score A (% pos. cells)	Score B (IHC signal intensity)	Final score (A + B)	Comments
Sham 1	0	0	0	Evaluation inconclusive, little IVD material left
Sham 2	5	3	8	Positive
DC 1	0	0	0	Evaluation inconclusive, little IVD material left
DC 2	5	3	8	Positive
DC 3	5	3	8	Positive

FIGURE 4 LDH, A, and relative PGE2, B, release 24 or 48 h after no (white bars) or 1 h (gray bars) of dynamic compression (DC) at 73 N (corresponding to 20% strain) and 0.5 Hz. n = 3; mean ± SD; **P < .01, ***P < .001
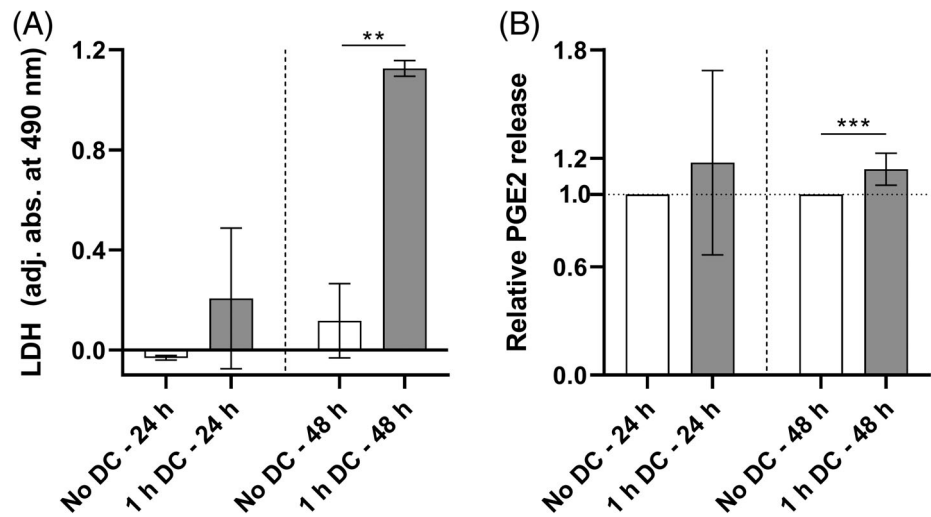
FIGURE 5 LDH, A, and relative PGE2, B, release 48 h after no (white bars) or 1 h (gray bars) of dynamic compression (DC) at 73 N (corresponding to 20% strain) and 0.5 Hz in the absence or presence (hatched bars) of 50 to 200 nM of the TRPV4 antagonist GSK2193874. n = 4; mean ± SD; *P < .05, ***P < .001
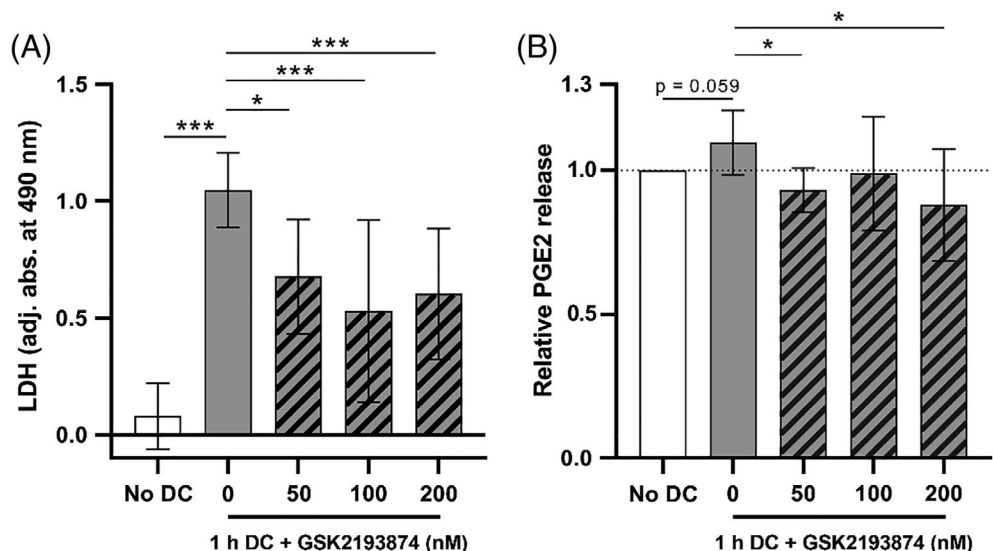
3.4 | TRPV4 inhibition decreases compression-induced LDH and PGE2 release in vitro

To test whether compression-induced cell damage and inflammation were mediated by TRPV4, we blocked the ion channel with the selective antagonist GSK2193874 at different concentrations (50 to 200 nM) during dynamic compression and measured LDH and PGE2 release 48 h after mechanical loading. Once again, LDH release was significantly increased in compressed samples compared to controls (Figure 5A). Interestingly, the compression-induced LDH release was partially but significantly reduced by TRPV4 inhibition at all GSK2193874 concentrations (Figure 5A). In this data set, the small
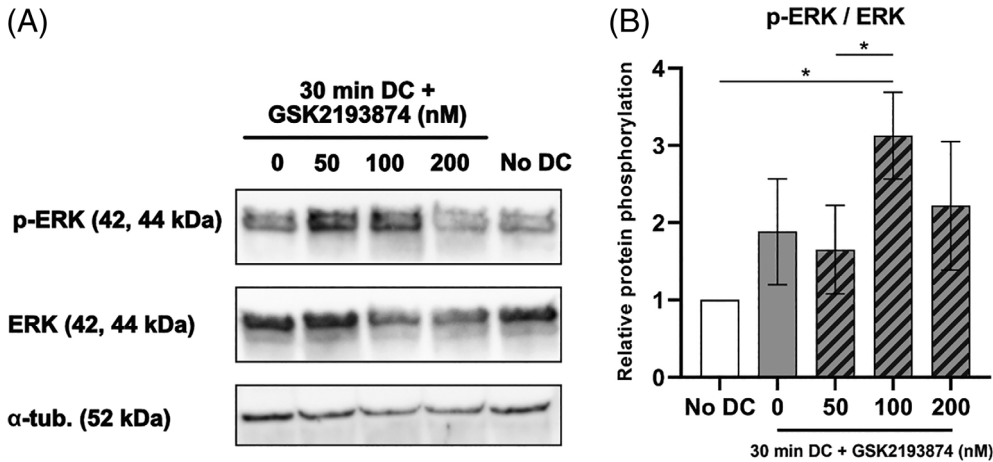
FIGURE 6 Representative Western blot, A, and densitometry analysis B, of phosphorylated and total ERK 1/2 immediately after no (white bar) or 30 min (gray bars) of dynamic compression (DC) at 73 N (corresponding to 20% strain) and 0.5 Hz in the absence or presence (hatched bars) of 50 to 200 nM of the TRPV4 antagonist GSK2193874. α-tubulin bands are shown as a loading control in A. n = 3; mean ± SD; *P < .05
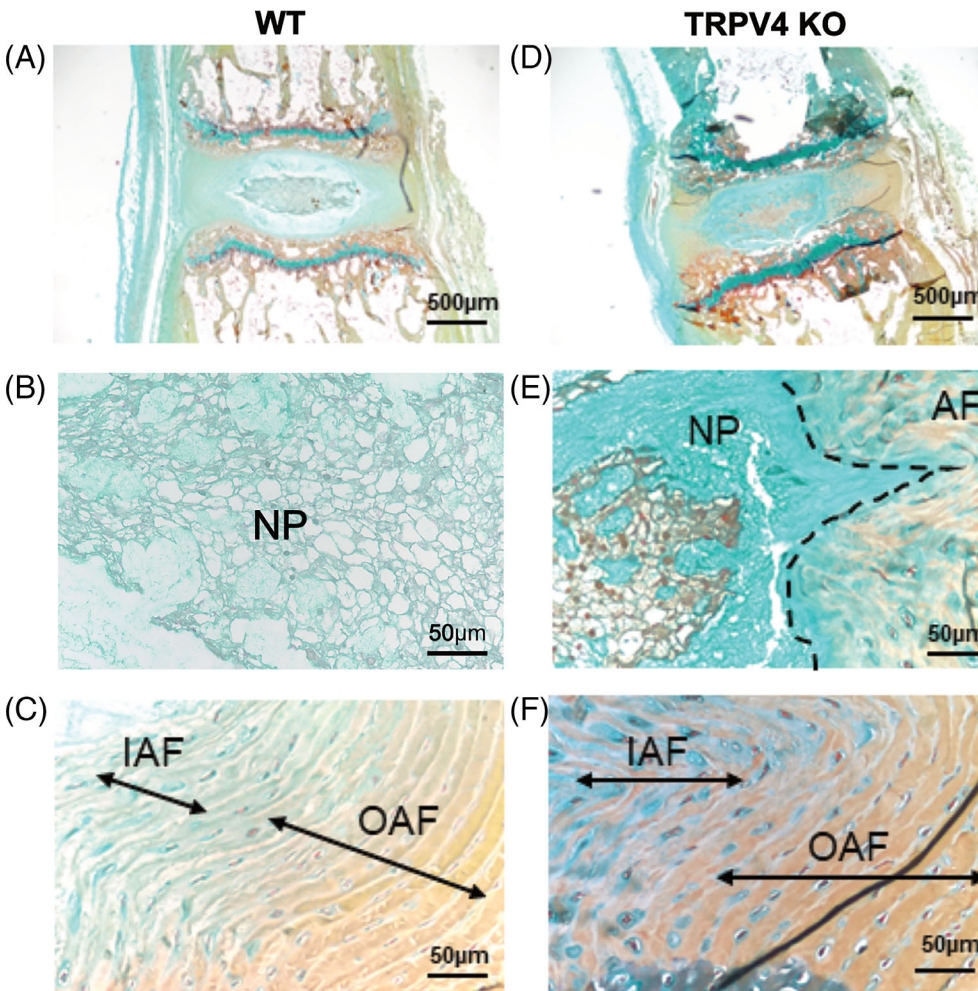
FIGURE 7 FAST staining of IVDs of wild-type (WT; A-C) and trpv4 knockout (KO; D-F) mouse tails. The nucleus pulposus (NP; B, E), inner and outer annulus fibrosus (IAF and OAF; C, F) are shown with a higher magnification. Scale bars: 500 μm in A, D; 50 μm in B, E, and C, F. n = 5
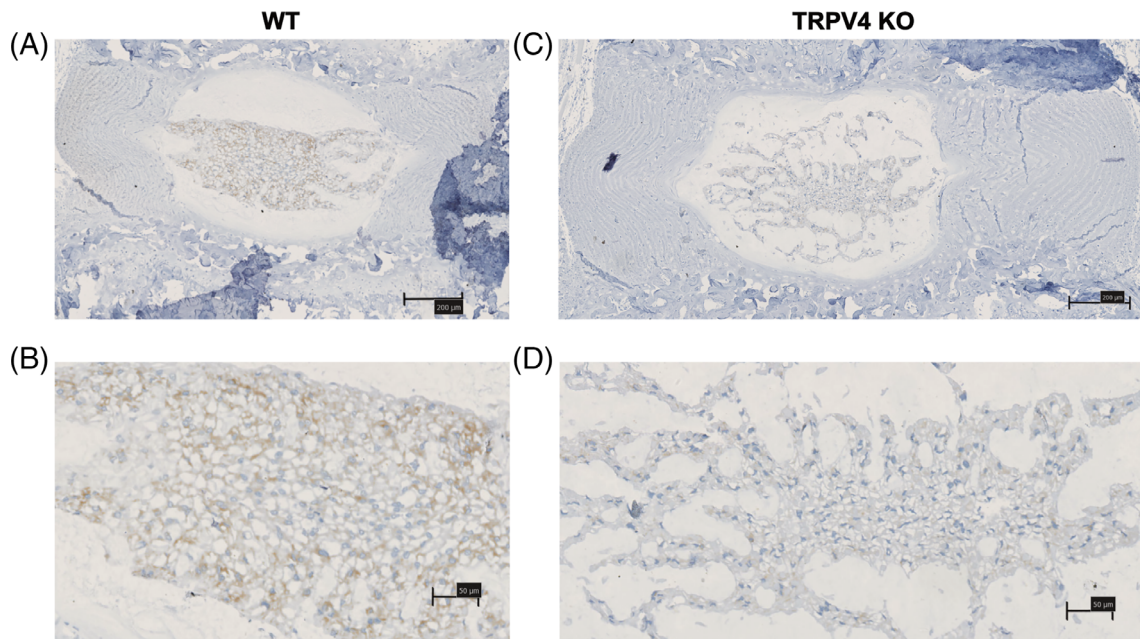
FIGURE 8 COX2 immunohistochemistry of IVDs of wild-type (WT; A, B) and trpv4 knockout (KO; C, D) mouse tails. Scale bars: 200 μm in A, C, and 50 μm in B, D. n = 3

TABLE 3 Allred scoring of COX2 immunohistochemistry of IVDs of wild-type (WT) and trpv4 knockout (KO) mouse tails

Sample	Score A (% pos. cells)	Score B (IHC signal intensity)	Final score (A + B)	Comments
WT 1	4	2	6	Positive
WT 2	4	2	6	Positive
WT 3	4	2	6	Positive
trpv4 KO 1	1	1	2	Negative
trpv4 KO 1	1	1	2	Negative
trpv4 KO 3	1	1	2	Negative

augmentation in PGE2 release induced by dynamic compression did not reach statistical significance ($P = .059$; Figure 5B). Nevertheless, the TRPV4 inhibitor significantly decreased PGE2 release at 50 and 200 nM compared to the compressed condition without antagonist (Figure 5B). The TRPV4 channel thus partially mediates compression-induced cell damage and inflammation, as measured by LDH and PGE2 release.

3.5 | TRPV4 inhibition during dynamic compression activates the ERK MAPK pathway

MAPKs are known to play a role in apoptosis, survival, and inflammation in IVDs.[18] In order to test whether dynamic compression activates MAPKs and whether TRPV4 is involved in MAPK regulation, we measured the expression of total and phosphorylated MAPKs after 30 min of compression in the absence or presence of TRPV4 antagonist.

Western blot bands for (p)-p38 and (p)-JNK were very faint or even absent and did not allow for densitometry analysis. However, (p)-ERK bands could be detected in all three tested cows. The expression of total ERK relative to the α-tubulin loading control remained similar across conditions (Figure 6A). Samples dynamically compressed for 30 min without TRPV4 inhibitor displayed denser bands for p-ERK compared to non-compressed controls in all animals (Figure 6A,B). However, upon densitometry analysis, the 1.88-fold increase in the p-ERK/ERK ratio compared to controls was not statistically significant (Figure 6B). Interestingly, blocking TRPV4 with 100 nM GSK2193874 during compression significantly increased ERK phosphorylation by 3.13-fold compared to non-compressed samples (Figure 6B). Moreover, ERK phosphorylation with 100 nM TRPV4 antagonist was significantly higher than with 50 nM (Figure 6B). These data show that TRPV4 inhibition during compression activates the ERK MAPK pathway.

3.6 | Trpv4 KO murine IVDs show mild degeneration compared to WT IVDs

In the last part of the study, and as a proof-of-concept, we verified the observed roles of the TRPV4 ion channel in IVD homeostasis and COX2 regulation in murine IVDs that were not loaded. We first stained IVDs from WT and trpv4 KO mice with the FAST technique. The structure of WT IVDs was unaltered (Figure 7A), with an intact NP (Figure 7B) surrounded by concentric AF lamellae (Figure 7 C). Nevertheless, IVDs of trpv4 KO mice showed a mildly degenerated phenotype (Figure 7D), characterized by a discontinued NP/AF boundary (Figure 7D,E), partial reversals of the AF lamellae into the NP (Figure 7D,E), and the presence of round chondrocyte-like cells at the transition between the NP and the inner AF (Figure 7E,F). These

images show that trpv4 KO promotes a mild degeneration in mouse IVDs, thus suggesting that TRPV4 plays a role in IVD homeostasis.

3.7 | Trpv4 KO murine IVDs show less COX2 expression in the NP compared to WT IVDs

We finally confirmed the link between TRPV4 and COX2 by performing IHC on WT and trpv4 KO mouse IVDs. COX2 was expressed in the NP of WT IVDs (Figure 8A,B), similarly to sham IVDs (Figure 3A,B) (Table 3). Interestingly, COX2 was not detected in trpv4 KO IVDs (Figure 8C,D) (Table 3). TRPV4 thus regulates COX2 expression in murine IVDs in vivo.

4 | DISCUSSION

Aberrant mechanical loading is a contributor to IVD degeneration, which can cause DDD and LBP. However, the underlying mechanosensing and mechanotransduction mechanisms are poorly understood. This lack of understanding prevents the development of drugs that specifically target the molecular players that are involved in these pathways.

In this study, we investigated whether the mechanosensitive TRPV4 ion channel mediates the transduction of hyperphysiological dynamic compression in murine IVDs in vivo and bovine NP cells in vitro. We report novel evidence that compression-induced NP cell damage and inflammation are reduced by TRPV4 pharmacological inhibition, which might promote cell survival via the activation of the ERK MAPK pathway.

Our data show that hyperphysiological dynamic compression has degenerative effects both in vivo and in vitro. Short repetitive dynamic compression at 8 N, 2 Hz over 4 weeks provoked mild degeneration in murine caudal IVDs in vivo, as shown by FAST histological staining. These results agree with previous studies that showed that hyperphysiological dynamic compression (at high magnitude, frequency, or duration) causes IVD degeneration in rodent in vivo models.[8,11,12,14,16] Interestingly, dynamic compression did not affect COX2 expression in vivo. We speculate that this lack of change might be due to the short hyperphysiological loading of 5 min per day. The study should be repeated with a longer loading duration per day, and COX2 activity should be evaluated to determine the link between hyperphysiological dynamic compression and COX2 expression/activity. Our in vitro model, which is constituted of bovine NP cells embedded in a matrix-mimicking agarose-collagen hydrogel, recapitulated the detrimental changes induced by dynamic compression in vivo. Hyperphysiological dynamic compression of the cell-laden scaffolds caused a considerable increase in the release of LDH, an indicator of cell damage, and a slight augmentation in the release of PGE2, a product of COX2. We speculate that repetitive mechanical stimulation (instead of a single continuous loading of 1 h) might increase the small increase in PGE2 release. The effects of compression were time-dependent, as they were detected 48 h after the end of mechanical

loading but not after 24 h. Previous studies have similarly shown cell death and increase in inflammatory mediators as a result of hyperphysiological dynamic compression.[8-10]

The novel findings that TRPV4 inhibition attenuates compression-induced LDH and PGE2 release in vitro, and that TRPV4 KO induces IVD degeneration and reduced COX2 expression in vivo, suggest a dual role of TRPV4 in the IVD. On one hand, our data show that TRPV4 pharmacological inhibition significantly reduces cell damage and inflammation induced by hyperphysiological dynamic compression. While these findings are new in NP cells, they find an echo in other studies showing that induced cell death is mitigated by TRPV4 inhibition or knockdown in other organs and tissues such as pancreas, brain and heart.[35-38] Moreover, TRPV4 inhibition was shown to prevent increases in PGE2 release induced by hypo-osmotic stimulation in porcine articular chondrocytes.[39] We also previously showed that stretch-induced inflammation (including increased COX2 mRNA expression and PGE2 release) was partially TRPV4-dependent in AF cells.[24] The reduction in PGE2 release caused by TRPV4 inhibition in vitro is in further agreement with our in vivo data showing a decreased COX2 expression in the NP of trpv4-deficient mice. On the other hand, TRPV4 expression is necessary and plays a role in IVD homeostasis. Trpv4 KO murine IVDs displayed mild degeneration compared to WT IVDs. These results align with previous reports of trpv4-deficient mice exhibiting mildly detrimental phenotypes, including a larger bladder capacity due to impaired mechanosensing, thicker bones due to impaired osteoclast differentiation, reduced water intake due to altered osmosensing, and compromised pressure and pain sensing.[40] While the constitutive expression of TRPV4 seems to be essential throughout the body, its temporary inhibition or conditional downregulation in the IVD might counteract exacerbated mechanosensing and pain induced by aberrant mechanical stress during DDD and LBP. Nevertheless, experiments with mechanical loading of trpv4 KO and WT mouse tails should be performed to confirm these results.

Finally, our finding that TRPV4 inhibition during dynamic compression activates the ERK MAPK pathway supports a role of TRPV4 in cell death. In fact, the ERK pathway is known to regulate survival and apoptosis in IVD cells and tissues.[18,41,42] Moreover, ERK activation was previously shown to counteract compression-induced apoptosis in the endplate and transitional zone of the AF in mouse IVDs.[18,41] Our results are in further agreement with previous studies that demonstrate a link between TRPV4 and ERK. Hdud and colleagues showed that hypo-osmotic stress increased the expression of TRPV4 in equine articular chondrocytes.[43] Inhibition of ERK prevented the increase of TRPV4 expression in hypo-osmotic conditions and reduced TRPV4 expression in iso-osmotic conditions compared to controls.[43] Moreover, TRPV4 inhibition was previously shown to reduce myocardial ischemia/reperfusion injury in mice by attenuating apoptosis and increasing ERK phosphorylation.[38] Our results suggest that TRPV4 mediates compression-induced cell damage/death, as TRPV4 inhibition reduces LDH signal during compression (ie, reduces cytotoxicity). Moreover, TRPV4 inhibition also phosphorylates ERK, which we interpret as a pro-survival signal in this context.

The conclusions of this study are limited by several aspects. First, two different animal models were used. While the mouse is an excellent model to investigate mechanical loading, the small size of murine IVDs prevents harvesting a sufficient amount of IVD cells for in vitro experiments. High amounts of NP cells were required for embedding in agarose-collagen hydrogels, and this quantity could also not be achieved by expansion of human NP cells, due to their low availability and proliferation rate. Moreover, while female mice were used in compression experiments, male WT and trpv4 KO mice were used later, thus preventing a direct comparison between the two data sets. Next, although the in vivo and in vitro loading regimes both have a hyperphysiological loading magnitude, a physiological frequency, and the same overall duration, they differ in the fact that the in vivo loading is repetitive and the in vitro loading is continuous. This difference can explain different observations between the two experimental settings. Finally, the agarose-collagen in vitro model is composed of collagen I instead of collagen II, which would mimic better the composition of the healthy NP extracellular matrix. The reason for this is that collagen II is about 40 times more expensive than collagen I and is provided at a very diluted concentration of 0.5 mg/mL (https://advancedbiomatrix.com/). Collagen II is normally recognized by discoidin domain receptor 2 (DDR2), which also recognizes collagen I with high affinity.[44] We speculate that the DDR2 pathway might therefore still be recapitulated in our hydrogels through collagen I binding. Additionally, collagen I might activate other pathways (eg, integrin-mediated ones). However, this might not be a major drawback, as the NP also contains collagen I, although at a smaller proportion compared to collagen II.[45]

In summary, we show that TRPV4 regulates COX2/PGE2 in bovine NP cells in vitro and in mouse IVDs in vivo, and that TRPV4 inhibition significantly reduces cell damage and PGE2 release induced by hyperphysiological compression in vitro, possibly via ERK activation. These novel findings thus identify TRPV4 as a promising therapeutic target to treat IVD degeneration, DDD, and LBP. Preclinical and clinical trials examining TRPV4 inhibition in the context of DDD and LBP are currently lacking. However, the administration of the TRPV4 antagonist GSK2798745 to healthy volunteers and heart failure patients was recently shown to be safe.[46] Targeting the mechanosensitive TRPV4 channel may benefit patients with IVD pathologies caused by aberrant mechanical loading. Nevertheless, it should be noted that TRPV4 is polymodal, ubiquitous, and its constitutive expression seems to be necessary. Therefore, a therapy targeting TRPV4 needs to be carefully elaborated in order to maintain its beneficial and necessary roles in homeostasis. A localized and/or temporary inhibition or knockdown (eg, via the CRISPR-based technology[47]) of TRPV4 in the IVD, via injection of a specific antagonist or inducible gene editing in case of excessive mechanical load, might be desirable therapeutic strategies in the future.

ACKNOWLEDGMENTS

CONFLICT OF INTEREST

All authors declare no conflict of interest.

AUTHOR CONTRIBUTIONS

Elena Cambria conceived the project, designed and conducted experiments, analyzed data, and wrote the manuscript. Sally Heusser conducted in vitro experiments. Ariane C. Scheuren designed and conducted mouse mechanical loading experiments. Wai Kit Tam performed and analyzed FAST histological staining. Agnieszka A. Karol optimized and analyzed COX2 immunohistochemistry. Wolfgang Hitzl performed statistical analysis. Victor Y. Leung supervised FAST histological staining. Ralph Müller designed and supervised mouse loading experiments. Stephen J. Ferguson and Karin Wuertz-Kozak provided funding and supervised the project. All authors reviewed and approved the manuscript.

ORCID

Elena Cambria https://orcid.org/0000-0001-6896-5421
Karin Wuertz-Kozak https://orcid.org/0000-0002-3281-4629

REFERENCES

1. Adams MA, Roughley PJ. What is intervertebral disc degeneration, and what causes it? *Spine*. 2006;*31*(18):2151-2161.
2. Vergroesen PPA, Kingma I, Emanuel KS, et al. Mechanics and biology in intervertebral disc degeneration: a vicious circle. *Osteoarthr Cartil*. 2015;*23*(7):1057-1070.
3. Airaksinen O, Brox JI, Cedraschi C, et al. European guidelines for the management of chronic nonspecific low back pain. *European Spine J*. 2006;*15*:S192-S300.
4. Balague F, Mannion AF, Pellise F, Cedraschi C. Non-specific low back pain. *Lancet*. 2012;*379*(9814):482-491.
5. Chan SC, Ferguson SJ, Gantenbein-Ritter B. The effects of dynamic loading on the intervertebral disc. *Eur Spine J*. 2011;*20*(11):1796-1812.
6. Bao S. Mechanical stress. *Handb Clin Neurol*. 2015;*131*:367-396.
7. Fearing BV, Hernandez PA, Setton LA, Chahine NO. Mechanotransduction and cell biomechanics of the intervertebral disc. *JOR Spine*. 2018;*1*(3):e1026.
8. Walsh AJ, Lotz JC. Biological response of the intervertebral disc to dynamic loading. *J Biomech*. 2004;*37*(3):329-337.
9. Wang DL, Jiang SD, Dai LY. Biologic response of the intervertebral disc to static and dynamic compression in vitro. *Spine (Phila pa 1976)*. 2007;*32*(23):2521-2528.
10. Illien-Junger S, Gantenbein-Ritter B, Grad S, et al. The combined effects of limited nutrition and high-frequency loading on intervertebral discs with endplates. *Spine (Phila pa 1976)*. 2010;*35*(19):1744-1752.
11. MacLean JJ, Lee CR, Grad S, Ito K, Alini M, Iatridis JC. Effects of immobilization and dynamic compression on intervertebral disc cell gene expression in vivo. *Spine (Phila pa 1976)*. 2003;*28*(10):973-981.
12. Ching CT, Chow DH, Yao FY, Holmes AD. Changes in nuclear composition following cyclic compression of the intervertebral disc in an in vivo rat-tail model. *Med Eng Phys*. 2004;*26*(7):587-594.
13. Korecki CL, Kuo CK, Tuan RS, Iatridis JC. Intervertebral disc cell response to dynamic compression is age and frequency dependent. *J Orthop Res*. 2009;*27*(6):800-806.

14. Maclean JJ, Lee CR, Alini M, Iatridis JC. Anabolic and catabolic mRNA levels of the intervertebral disc vary with the magnitude and frequency of in vivo dynamic compression. *J Orthop Res*. 2004;*22*(6): 1193-1200.

15. MacLean JJ, Lee CR, Alini M, Iatridis JC. The effects of short-term load duration on anabolic and catabolic gene expression in the rat tail intervertebral disc. *J Orthop Res*. 2005;*23*(5):1120-1127.

16. Wuertz K, Godburn K, MacLean JJ, et al. In vivo remodeling of intervertebral discs in response to short- and long-term dynamic compression. *J Orthop Res*. 2009;*27*(9):1235-1242.

17. Kerr GJ, Veras MA, Kim MK, Seguin CA. Decoding the intervertebral disc: unravelling the complexities of cell phenotypes and pathways associated with degeneration and mechanotransduction. *Semin Cell Dev Biol*. 2017;*62*:94-103.

18. Wuertz K, Vo N, Kletsas D, Boos N. Inflammatory and catabolic signalling in intervertebral discs: the roles of NF-kappaB and MAP kinases. *Eur Cell Mater*. 2012;*23*:103-119.

19. Krupkova O, Zvick J, Wuertz-Kozak K. The role of transient receptor potential channels in joint diseases. *Eur Cells Mater*. 2017;*34*: 180-201.

20. Walter BA, Purmessur D, Moon A, et al. Reduced tissue osmolarity increases TRPV4 expression and pro-inflammatory cytokines in intervertebral disc cells. *Eur Cell Mater*. 2016;*32*:123-136.

21. Franco-Obregon A, Cambria E, Greutert H, et al. TRPC6 in simulated microgravity of intervertebral disc cells. *Eur Spine J*. 2018;*27*(10): 2621-2630.

22. Kameda T, Zvick J, Vuk M, et al. Expression and activity of TRPA1 and TRPV1 in the intervertebral disc: association with inflammation and matrix remodeling. *Int J Mol Sci*. 2019;*20*(7):1767.

23. Sadowska A, Hitzl W, Karol A, et al. Differential regulation of TRP channel gene and protein expression by intervertebral disc degeneration and back pain. *Sci Rep-Uk*. 2019;*9*:18889.

24. Cambria E, Arlt MJE, Wandel S, et al. TRPV4 inhibition and CRISPR-Cas9 knockout reduce inflammation induced by Hyperphysiological stretching in human annulus Fibrosus cells. *Cell*. 2020;*9*(7):1736.

25. O'Conor CJ, Leddy HA, Benefield HC, Liedtke WB, Guilak F. TRPV4-mediated mechanotransduction regulates the metabolic response of chondrocytes to dynamic loading. *P Natl Acad Sci USA*. 2014;*111*(4):1316-1321.

26. O'Conor CJ, Ramalingam S, Zelenski NA, et al. Cartilage-specific knockout of the Mechanosensory Ion Channel TRPV4 decreases age-related osteoarthritis. *Sci Rep-Uk*. 2016;*6*:29053.

27. Cambria E, Brunner S, Heusser S, et al. Cell-laden agarose-collagen composite hydrogels for Mechanotransduction studies. *Front Bioeng Biotechnol*. 2020;*8*:346.

28. Scheuren AC, Vallaster P, Kuhn GA, et al. Mechano-regulation of trabecular bone adaptation is controlled by the local in vivo environment and logarithmically dependent on loading frequency. *Front Bioeng Biotechnol*. 2020;*8*(1211):566346.

29. Webster DJ, Morley PL, van Lenthe GH, Muller R. A novel in vivo mouse model for mechanically stimulated bone adaptation–a combined experimental and computational validation study. *Comput Methods Biomech Biomed Engin*. 2008;*11*(5):435-441.

30. Leung VY, Chan WC, Hung SC, Cheung KM, Chan D. Matrix remodeling during intervertebral disc growth and degeneration detected by multichromatic FAST staining. *J Histochem Cytochem*. 2009;*57*(3): 249-256.

31. Tam V, Chan WCW, Leung VYL, et al. Histological and reference system for the analysis of mouse intervertebral disc. *J Orthop Res*. 2018; *36*(1):233-243.

32. Fedchenko N, Reifenrath J. Different approaches for interpretation and reporting of immunohistochemistry analysis results in the bone tissue - a review. *Diagn Pathol*. 2014;*9*:221.

33. Pratsinis H, Papadopoulou A, Neidlinger-Wilke C, Brayda-Bruno M, Wilke HJ, Kletsas D. Cyclic tensile stress of human annulus fibrosus cells induces MAPK activation: involvement in proinflammatory gene expression. *Osteoarthr Cartil*. 2016;*24*(4):679-687.

34. Moore C, Cevikbas F, Pasolli HA, et al. UVB radiation generates sunburn pain and affects skin by activating epidermal TRPV4 ion channels and triggering endothelin-1 signaling. *Proc Natl Acad Sci U S A*. 2013;*110*(34):E3225-E3234.

35. Casas S, Novials A, Reimann F, Gomis R, Gribble FM. Calcium elevation in mouse pancreatic beta cells evoked by extracellular human islet amyloid polypeptide involves activation of the mechanosensitive ion channel TRPV4. *Diabetologia*. 2008;*51*(12):2252-2262.

36. Bai JZ, Lipski J. Differential expression of TRPM2 and TRPV4 channels and their potential role in oxidative stress-induced cell death in organotypic hippocampal culture. *Neurotoxicology*. 2010;*31*(2):204-214.

37. Shi M, Du F, Liu Y, et al. Glial cell-expressed mechanosensitive channel TRPV4 mediates infrasound-induced neuronal impairment. *Acta Neuropathol*. 2013;*126*(5):725-739.

38. Dong Q, Li J, Wu QF, et al. Blockage of transient receptor potential vanilloid 4 alleviates myocardial ischemia/reperfusion injury in mice. *Sci Rep-Uk*. 2017;*7*:42678.

39. Phan MN, Leddy HA, Votta BJ, et al. Functional characterization of TRPV4 as an osmotically sensitive ion channel in porcine articular chondrocytes. *Arthritis Rheum*. 2009;*60*(10):3028-3037.

40. Nilius B, Voets T. The puzzle of TRPV4 channelopathies. *EMBO Rep*. 2013;*14*(2):152-163.

41. Ariga K, Yonenobu K, Nakase T, et al. Mechanical stress-induced apoptosis of endplate chondrocytes in organ-cultured mouse intervertebral discs: an ex vivo study. *Spine (Phila pa 1976)*. 2003;*28*(14): 1528-1533.

42. Risbud MV, Guttapalli A, Albert TJ, Shapiro IM. Hypoxia activates MAPK activity in rat nucleus pulposus cells: regulation of integrin expression and cell survival. *Spine (Phila pa 1976)*. 2005;*30*(22):2503-2509.

43. Hdud IM, Mobasheri A, Loughna PT. Effect of osmotic stress on the expression of TRPV4 and BKCa channels and possible interaction with ERK1/2 and p38 in cultured equine chondrocytes. *Am J Physiol-Cell Ph*. 2014;*306*(11):C1050-C1057.

44. Leitinger B, Steplewski A, Fertala A. The D2 period of collagen II contains a specific binding site for the human discoidin domain receptor, DDR2. *J Mol Biol*. 2004;*344*(4):993-1003.

45. Eyre DR, Muir H. Quantitative analysis of types I and II collagens in human intervertebral discs at various ages. *Biochim Biophys Acta*. 1977;*492*(1):29-42.

46. Goyal N, Skrdla P, Schroyer R, et al. Clinical pharmacokinetics, safety, and tolerability of a novel, first-in-class TRPV4 Ion Channel inhibitor, GSK2798745, in healthy and heart failure subjects. *Am J Cardiovasc Drug*. 2019;*19*(3):335-342.

47. Krupkova O, Cambria E, Besse L, Besse A, Bowles R, Wuertz-Kozak K. The potential of CRISPR/Cas9 genome editing for the study and treatment of intervertebral disc pathologies. *JOR Spine*. 2018;*1* (1):e1003.

SUPPORTING INFORMATION

Additional supporting information may be found online in the Supporting Information section at the end of this article.

How to cite this article: Cambria E, Heusser S, Scheuren AC, et al. TRPV4 mediates cell damage induced by hyperphysiological compression and regulates COX2/PGE2 in intervertebral discs. *JOR Spine*. 2021;4:e1149. https://doi.org/10.1002/jsp2.1149